JACS
JOURNAL OF THE AMERICAN CHEMICAL SOCIETY

Article

pubs.acs.org/JACS

Mechanistic Elucidation of Zirconium-Catalyzed Direct Amidation

Helena Lundberg,[†] Fredrik Tinnis,[†,⊥] Jiji Zhang,[†,⊥] Andrés G. Algarra,[†,‡] Fahmi Himo,*[,†] and Hans Adolfsson*[,†,§]

[†]Department of Organic Chemistry, Arrhenius Laboratory, Stockholm University, SE-106 91 Stockholm, Sweden

[‡]Departamento de Ciencia de los Materiales e Ingeniería Metalúrgica y Química Inorgánica, Universidad de Cádiz, Campus Universitario de Puerto Real, 11510 Puerto Real, Spain

[§]Department of Chemistry, Umeå University, SE-901 87 Umeå, Sweden

Supporting Information

ABSTRACT: The mechanism of the zirconium-catalyzed condensation of carboxylic acids and amines for direct formation of amides was studied using kinetics, NMR spectroscopy, and DFT calculations. The reaction is found to be first order with respect to the catalyst and has a positive rate dependence on amine concentration. A negative rate dependence on carboxylic acid concentration is observed along with S-shaped kinetic profiles under certain conditions, which is consistent with the formation of reversible off-cycle species. Kinetic experiments using reaction progress kinetic analysis protocols demonstrate that inhibition of the catalyst by the amide product can be avoided using a high amine concentration. These insights led to the design of a reaction protocol with improved yields and a decrease in catalyst loading. NMR spectroscopy provides important details of the nature of the zirconium catalyst and serves as the starting point for a theoretical study of the catalytic cycle using DFT calculations. These studies indicate that a dinuclear zirconium species can catalyze the reaction with feasible energy barriers. The amine is proposed to perform a nucleophilic attack at a terminal η^2-carboxylate ligand of the zirconium catalyst, followed by a C−O bond cleavage step, with an intermediate proton transfer from nitrogen to oxygen facilitated by an additional equivalent of amine. In addition, the DFT calculations reproduce experimentally observed effects on reaction rate, induced by electronically different substituents on the carboxylic acid.

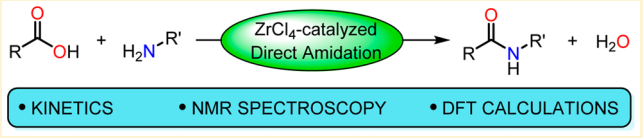

1. INTRODUCTION

Amides constitute a highly important substance class for a range of areas and applications such as pharmaceuticals, agrochemicals, materials, and food additives. In nature, enzymes catalyze the condensation of carboxylic acids and amines to form amides. For example, the templated ribosomal synthesis of polypeptides, known as translation, utilizes peptidyl transferase to connect the growing peptide chain with the correct amino acid, present in the ribosome as a tRNA ester.[1] Another example is glutamine synthetase that participates in metabolic regulation by catalyzing glutamine formation from glutamate and ammonia via an acyl−phosphate intermediate.[2] In the synthetic laboratory, amides are typically formed stoichiometrically via aminolysis of an activated carboxylic acid, commonly in the form of an acid halide or by the aid of a coupling reagent. This fact was clearly illustrated in a survey performed by three major pharmaceutical companies, showing that 93% of the N-acylations in the synthesis of 128 drug candidates were carried out by stoichiometric activation of the carboxylic acid.[3] This trend was recently confirmed in a review on large-scale amidation processes for the synthesis of pharmaceuticals, in which only a handful of catalytic protocols were employed.[4] However efficient, the activation/aminolysis strategy of a carboxylic acid inevitably generates at least stoichiometric amounts of waste in the process and introduces extra steps to the synthesis, along with the need for additional purifications. The formation of amides using atom-economical reagents has been highlighted by the ACS Pharmaceutical Roundtable as one of the areas where method development is much needed.[5]

Amides can be formed from several classes of starting compounds,[6] where carboxylic acids are generally considered the most challenging due to the acid−base reaction that can occur between the acid and the amine. The salt formation can be overcome by elevated reaction temperature (80−160 °C) at which moderate to good yields of amides can be obtained, depending on the substrates in use.[7] However, the high temperatures typically required are not suitable for highly functionalized or sensitive substrates and limit the applicability of thermal amidation. For this reason, catalysis is an attractive alternative to enable atom-economical formation of amides under milder conditions. Today, a limited number of catalytic protocols are known for the direct amidation of carboxylic acids and amines, mainly based on Lewis acidic boron compounds and early transition metal complexes.[8,9]

We have previously reported that several group IV metal complexes are efficient catalysts for the amidation of non-activated carboxylic acids under mild conditions.[10−12] The zirconium-catalyzed system[11a] is cost-efficient, requires low catalyst loadings, and results in high yields of product without

Received: October 20, 2016
Published: January 19, 2017

DOI: 10.1021/jacs.6b10973
J. Am. Chem. Soc. 2017, 139, 2286−2295

racemization of stereocenters in the vicinity of the reacting centers (Scheme 1). However, the mechanistic action of this

Scheme 1. Direct Zirconium-Catalyzed Amidation of Carboxylic Acids and Amines[11a]

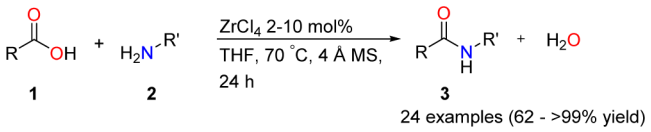

and similar metal-catalyzed systems is yet obscure. A detailed profiling of the reaction would improve the fundamental understanding of the mechanism for this type of early transition-metal-catalyzed amidation and, in turn, enable both the development of more efficient reaction protocols as well as provide clues for future development of new catalysts.

Herein, we present a mechanistic study based on kinetics, NMR spectroscopy, and density functional theory (DFT) calculations that provides unprecedented insight into zirconium-catalyzed direct amidation. We also demonstrate how the mechanistic understanding is employed in the reaction design that leads to improved yields and lower catalyst loadings.

2. RESULTS AND DISCUSSION

2.1. Kinetic Study. The reaction rate dependence on the different reaction components was studied in a series of experiments that were sampled and analyzed by ^{1}H NMR. Since alcohols were previously shown to quench the amidation reaction,[11a] the samples were injected directly into MeOD-d_4 and subjected to analysis without further workup. Phenylacetic acid (**1a**) and benzylamine (**2a**) were used as model substrates for the reactions. Activated powdered molecular sieves with a pore size of 4 Å were used to scavenge water formed in the reaction and thereby enable good yields of amide products.[11a] The thermal uncatalyzed formation of amide had previously been observed to be slow (13% isolated yield of amide **3a** after 24 h)[11a] and was determined to be insignificant for the present kinetic study. The NMR data displayed high reproducibility and were validated by good correlation between the conversion determined by ^{1}H NMR and the conversion calculated from the mass yield of identical reactions stopped at different times (see Supporting Information).

Figure 1 displays the kinetic profiles for three reactions using different catalyst concentrations with the same initial concentrations of **1a** and **2a**. As expected, the amidation

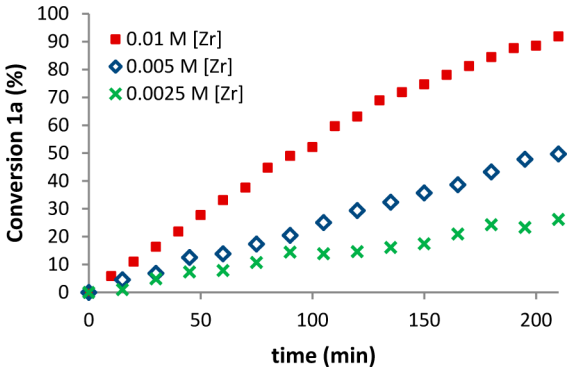

Figure 1. Kinetic profiles for three experiments using different catalyst concentrations. $[\mathbf{1a}]_o$ = 0.4 M, $[\mathbf{2a}]_o$ = 0.8 M.

process was found to be positive order in the catalyst concentration. An elegant graphical analysis method to determine the reaction order in the catalyst was recently presented by Burés.[13] It was demonstrated that temporal concentration data from reactions with identical initial molar concentrations of starting materials and different catalyst concentrations overlay when the time unit is multiplied by the catalyst concentration to the power of the reaction order and plotted versus molar concentration of the starting material. When this methodology was applied to the three reactions in Figure 1, the data were found to overlay well when the reaction order with respect to catalyst was set to 1 (Figure 2). This

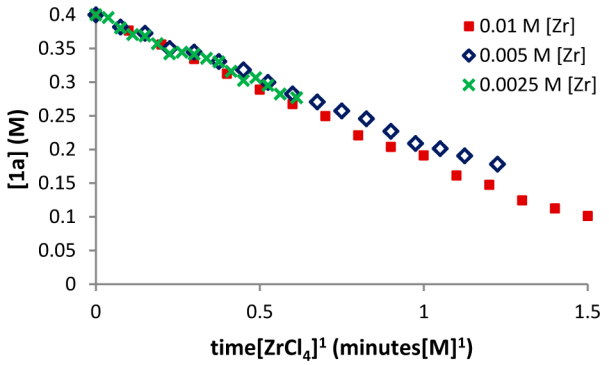

Figure 2. Kinetic profiles for three different catalyst concentrations plotted with a catalyst order of 1, using Burés' graphical analysis.[13] $[\mathbf{1a}]_o$ = 0.4 M, $[\mathbf{2a}]_o$ = 0.8 M.

behavior suggests a first-order rate dependence on the zirconium catalyst in this concentration range. The first-order rate dependence on [catalyst] is consistent with any nuclearity of the zirconium catalyst as long as it does not change during the catalytic cycle, for example, by going from monomer to dimer.[13,14] At zirconium concentrations ≥0.02 M, the kinetic profiles adopt a sigmoidal shape that suggests the formation of off-cycle species (vide infra). This complicates the use of Burés graphical method at these catalyst concentrations (see Supporting Information).

Blackmond and co-workers have developed powerful kinetic methods for mechanistic elucidation, known as the reaction progress kinetic analysis (RPKA) methodology.[15,16] One highly useful procedure within RPKA is referred to as the "same excess" protocol, designed to test the robustness of the catalyst under synthetically relevant conditions. The introduction of a parameter called "excess", defined as the molar difference in initial substrate concentrations, enables kinetic information to be obtained from experiments using the same excess of one reactant to the other. Graphical time adjustment of the temporal concentration data will cause two same excess experiments to overlay if the concentration of active catalyst is constant over the course of the reaction. Applying the same excess protocol to the amidation reaction, it becomes clear that the curves do not overlay and that the rate by which [**1a**] decreases is higher in the experiment with lower initial reactant concentrations (Figure 3). This observation indicates that the concentration of active catalyst decreases with performed turnovers, due to either inhibition or deactivation.

To probe the origins of the decrease in active catalyst concentration, a third same excess experiment was performed. Product **3a** was added at the outset of the experiment to fully mimic the conditions for the initial reaction at 25% conversion.

DOI: 10.1021/jacs.6b10973
J. Am. Chem. Soc. 2017, 139, 2286−2295

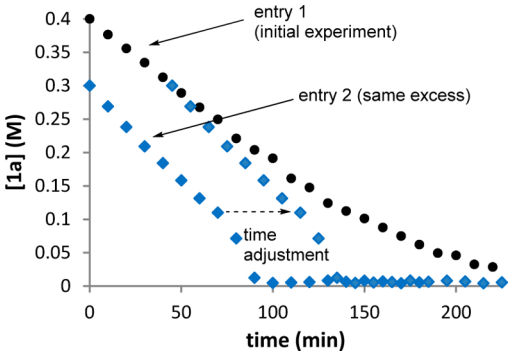

Figure 3. Kinetic profiles for the same excess reactions in Table 1, entries 1 and 2.

As can be seen in Figure 4, the time-adjusted curve for the third same excess experiment overlays well with the initial experiment, clearly demonstrating that the catalyst is sensitive toward product inhibition. Furthermore, the results demonstrate that the catalyst is stable under the applied conditions and not affected by deactivation processes such as hydrolysis and subsequent precipitation of zirconia.[17]

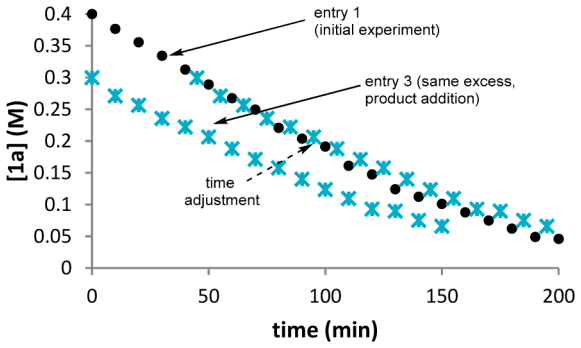

Figure 4. Kinetic profiles for the same excess reactions in Table 1, entries 1 and 3, indicating product inhibition.

However, the inhibition of active catalyst by the formed product is problematic since it puts a limit to how low catalyst loadings can be. We were therefore interested to see if the inhibition could be circumvented by alteration of the reaction conditions. Gratifyingly, when performing two same excess experiments with three times larger excess of amine (Table 1), product inhibition was no longer observed (Figure 5). This result indicates that the equilibrium for the amide association/dissociation to zirconium is affected by amine concentration, which is a vital piece of information for the design of a more efficient reaction protocol.

Table 1. Reagent Concentrations for the Same Excess Reactions in Figures 3–5

entry	[**1a**] (mol/L)	[**2a**] (mol/L)	[**3a**] (mol/L)	excess ([**2a**] − [**1a**])
1[a]	0.4	0.8	0	0.4
2[a]	0.3	0.7	0	0.4
3[a]	0.3	0.7	0.1	0.4
4[b]	0.4	1.6	0	1.2
5[b]	0.3	1.5	0	1.2

[a][Zr] = 0.01 M. [b][Zr] = 0.02 M.

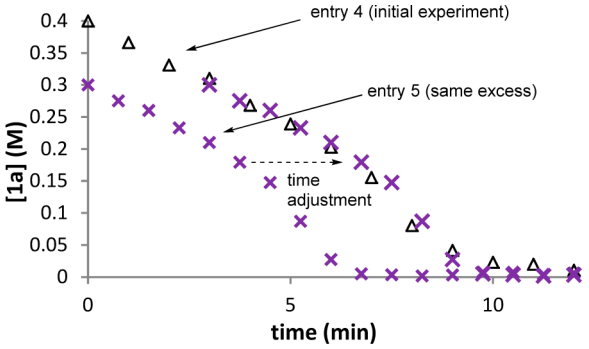

Figure 5. Kinetic profiles for the same excess reactions in Table 1, entries 4 and 5. No product inhibition of the catalyst is observed when a large excess of amine is used.

To gain more mechanistic information, the rate dependencies in [**1a**] and [**2a**] were studied in three experiments using different excesses of reactants at a constant catalyst concentration. As seen in Figure 6, the equimolar reaction (excess 0 M) displays an intermediate rate (red triangles). The reaction rate using the same [**1a**] and 0.4 M excess of **2a** is higher (blue squares), clearly demonstrating that the reaction exhibits positive rate dependence on [**2a**]. Surprisingly, the reaction with the initial concentration of **2a** and 0.2 M excess of **1a** (green circles) is slower compared to the equimolar reaction, indicating a negative rate dependence on [**1a**]. This unusual observation was confirmed by additional "different excess" experiments, performed with lower initial concentration of **1a** (see Supporting Information).

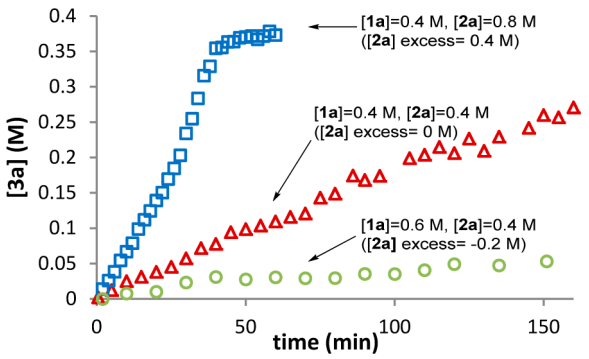

Figure 6. Kinetic profiles for three experiments using different initial concentrations of carboxylic acid **1a** and amine **2a**. [Zr] = 0.02 M.

A negative rate dependence on a substrate may at first seem counterintuitive but is often indicative of the formation of species that exist outside the catalytic cycle.[16,18−21] The acid−base equilibrium between the carboxylic acid and the amine (Scheme 2) is commonly thought to be a challenge for direct amidation due to the decreased nucleophilicity of a protonated amine. Indeed, the use of protonated amine was found to be detrimental to the zirconium-catalyzed amidation (Scheme 3).

To test whether the negative rate dependence on the carboxylic acid is caused by formation of ammonium

Scheme 2. Formation of an Ammonium Carboxylate Salt from Carboxylic Acid and Amine

DOI: 10.1021/jacs.6b10973
J. Am. Chem. Soc. 2017, 139, 2286−2295

Scheme 3. No Product Forms When Protonated 2a Is Used as Nucleophile

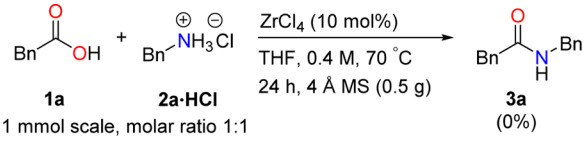

carboxylate, a series of experiments were carried out using a large excess of amine **2a** (3.52–3.92 M excess relative to [**1a**]). At this concentration, the amine is present in a 8- to 9-fold excess relative to the carboxylic acid and is therefore protonated only to a minor extent. Nevertheless, negative rate dependence on [**1a**] was still observed under these conditions (Figure 7),

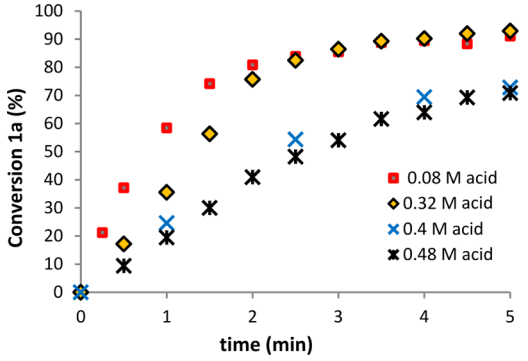

Figure 7. Reaction rate decreases as carboxylic acid concentration increases even in the presence of high [amine]. $[\mathbf{2a}]_o$ = 4.0 M, [Zr] = 0.02 M.

suggesting that the carboxylic acid inhibits the catalyst by the formation of an off-cycle species. Such formation can be reversible[16,20,21] or irreversible,[22] with both scenarios resulting in a decrease in the concentration of active catalyst and hence a lower reaction rate. Unproductive catalyst–substrate complexes have been called "parasitic species"[23] but have also been shown to protect the catalyst from irreversible deactivation in some cases.[20,21]

The positive rate dependence on [amine] observed in the different excess experiments in Figure 6 was further confirmed by another set of experiments (Figure 8). The sigmoidal shape of the kinetic profiles complicates the use of regular initial rate analysis for the determination of reaction orders. Nevertheless,

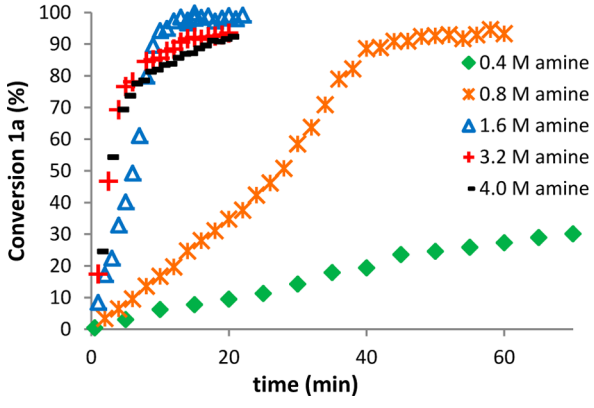

Figure 8. Reaction rate increases with amine concentration. $[\mathbf{1a}]_o$ = 0.4 M, [Zr] = 0.02 M.

Figure 8 indicates that a 2-fold increase in [amine] results in more than a 2-fold decrease in reaction time to reach a certain conversion, pointing toward a reaction order >1 in amine. Furthermore, the sigmoidal shape of the kinetic profiles provides clues regarding the mechanistic action of the system. Combined with the observed negative rate dependence on [carboxylic acid], the S shape of the kinetic profiles (Figure 8) provides support for the presence of reversible off-cycle species formed from catalyst and carboxylic acid.[19,21]

At the outset of the reaction, equilibrium is established between the catalyst–acid off-cycle reservoir and free reaction components that participate in the catalytic cycle. Since a portion of the catalyst has been siphoned off from the cycle, the starting concentration of active catalyst and hence the reaction rate is lower than that in theory. As the reaction proceeds, the concentration of free carboxylic acid decreases in the reaction mixture. This concentration change affects the equilibrium of the off-cycle catalyst–acid complex in accordance with Le Chatelier's principle, resulting in the release of carboxylic acid and catalyst. The increase in catalyst concentration enhances the reaction rate, which is observed as a section with steeper slope in the kinetic profile. At high conversions when the substrate concentration is low, the reaction rate slows down and the kinetic profile levels out. A schematic picture of the correlation between off-cycle species and catalytic cycle is found in Scheme 4.

Scheme 4. Schematic Picture of Off-Cycle Species in Equilibrium with Free Catalyst and Carboxylic Acid That Participate in the Catalytic Cycle

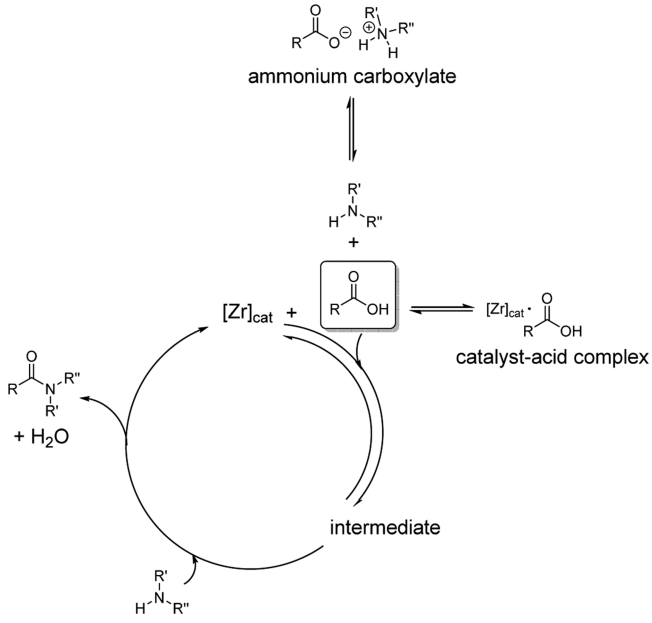

To test the influence of substituents on the reaction rate, a set of experiments was performed using differently substituted benzoic acids (Figure 9). Qualitative analysis of the kinetic profiles clearly indicates that electron-withdrawing groups are beneficial for the rate, something that was previously reported for Hf-catalyzed direct amidation.[12] The substituent effect could be explained by the electronic nature of the tetrahedral carbon. This carbon is expected to be electron-deficient due to its three bonds to electronegative atoms. An electron-withdrawing group on the phenyl ring will likely further

DOI: 10.1021/jacs.6b10973
J. Am. Chem. Soc. 2017, 139, 2286–2295

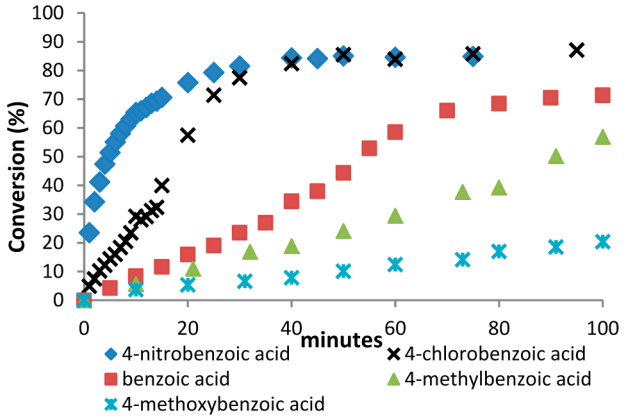

Figure 9. Kinetic profiles for substituted benzoic acids. $[\mathbf{1}]_o$ = 0.4 M, $[\mathbf{2a}]_o$ = 1.6 M, [Zr] = 0.02 M.

decrease the electron density of the central carbon, thus destabilizing the transition state structure and facilitating its collapse. This would, in turn, result in a lower barrier for the C−O bond breakage.

2.2. Optimized Reaction Protocols. The kinetic insights were utilized for the design of a more efficient reaction protocol for demanding substrates,[11a] including branched and secondary amines as well as an electron-rich carboxylic acid. The importance of the amine for several aspects of the reaction suggested that the use of >1 equiv of amine to carboxylic acid would result in higher product yields without the need for increased catalyst loading, reaction temperature, or time. Indeed, amides **3c−e** were isolated in 98, 96, and 82% yield, respectively, in batch experiments using 4 equiv of amine (1.6 M) after 19 h. These yields stand in stark contrast to those obtained in the equimolar reactions (22, 39, and 10%, respectively) (Scheme 5).

Scheme 5. Direct Amidation of Demanding Substrates

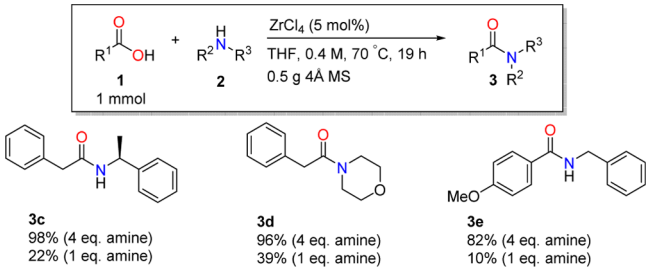

Furthermore, a higher amine concentration enabled us to decrease the catalyst loading. Using only 0.5 mol % of $ZrCl_4$, amide **3a** was isolated in 95% yield after 3 h (Scheme 6). Remaining amine can be retrieved by extractive workup of the reaction mixture.

Scheme 6. Efficient Direct Amidation of 1a Using a Decreased Catalyst loading

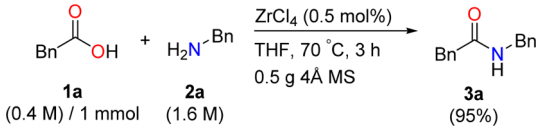

2.3. NMR Study. Zirconium chloride can be hydrolyzed in the presence of water to generate ZrO_2 and HCl.[17] ZrO_2 has previously been reported to be a poor direct amidation catalyst,[24] whereas a limited number of amidation protocols have been reported to use Brønsted acid catalysts under certain conditions.[8] To confirm that the amidation is not simply Brønsted-acid-catalyzed under our reaction conditions, a control experiment using 20 mol % of HCl (2 M in diethyl ether) was performed, resulting in an isolated yield of amide **3a** of 8% after 24 h. This result is comparable to the thermal catalyst-free background reaction (13% isolated yield)[11a] and clearly demonstrates that HCl is not the active catalyst.

To study the coordination of the carboxylic acid to zirconium under synthetically relevant conditions and probe the nature of the active amidation catalyst, a series of NMR experiments were carried out in THF-d_8 at 65 °C. Using ^{13}C(1)-labeled acetic acid (**^{13}C-1b**) and sodium acetate ([**^{13}C-1b**]$^-$**Na**$^+$) in two separate experiments, it was found that both species gave rise to a broadened carbon signal at 171.5 ppm when present in a 1:1 mixture with $ZrCl_4$ (see Supporting Information). The carboxyl carbon signal was assigned to a zirconium-bound acetate because such species are known to form upon mixing of a zirconium chloride complex and either neutral acetic acid or sodium acetate by formal displacement of HCl or NaCl, respectively.[25,26]

A carboxylate can bind as a terminal ligand to a metal center in monodentate η^1 binding mode as well as in chelating η^2 mode with both oxygens coordinated to the metal. In addition, the carboxylate can serve as a bridging μ-ligand connecting two metal centers (Figure 10).[27−29] Bidentate carboxylates are

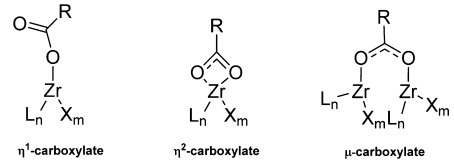

Figure 10. Carboxylates can ligate to Zr(IV) with different binding modes.

expected to display a higher ^{13}C NMR shift compared to that of monodentate analogues, due to the decreased electron density at the carboxylic carbon when both oxygens donate electrons to a metal center.[30]

This observation is interpreted as the formation of a zirconium complex with two coordinated acetates that ligate with different binding modes. By addition of a third equivalent of **2a**, the upfield signal (171.5 ppm) disappears, and the downfield peak broadens further and moves to a slightly higher shift (Figure 11E), suggesting that both acetates adopt a bidentate binding mode. The addition of more acid **^{13}C-1b** to the mixture did not render useful information due to precipitation in the NMR tube. This matter complicates the use of NMR to study the nature of the catalyst−acid off-cycle species, which is expected to contain higher ratios of carboxylic acid to zirconium compared to product-forming complexes. The nature of the off-cycle species is further discussed in section 2.4 (vide infra).

The formation of the broad downfield carboxylic carbon signal (182.5 ppm) was also observed upon addition of amine **2a** to the equimolar mixture of $ZrCl_4$ and ^{13}C-labeled sodium acetate [**^{13}C-1b**]$^-$**Na**$^+$ (see Supporting Information). In this case, however, only one amine equivalent was required

DOI: 10.1021/jacs.6b10973
J. Am. Chem. Soc. 2017, 139, 2286−2295

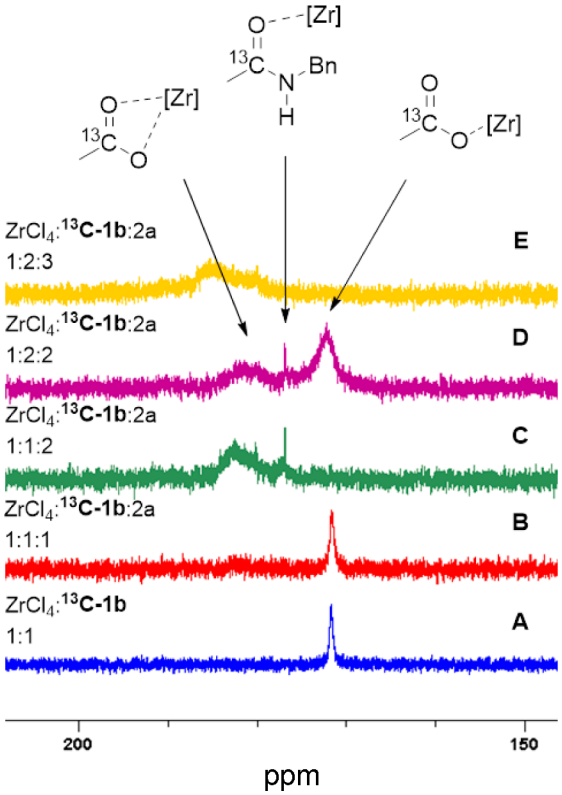

Figure 11. Carbonyl signal changes as more carboxylic acid ^{13}**C-1b** and amine **2a** are added sequentially.

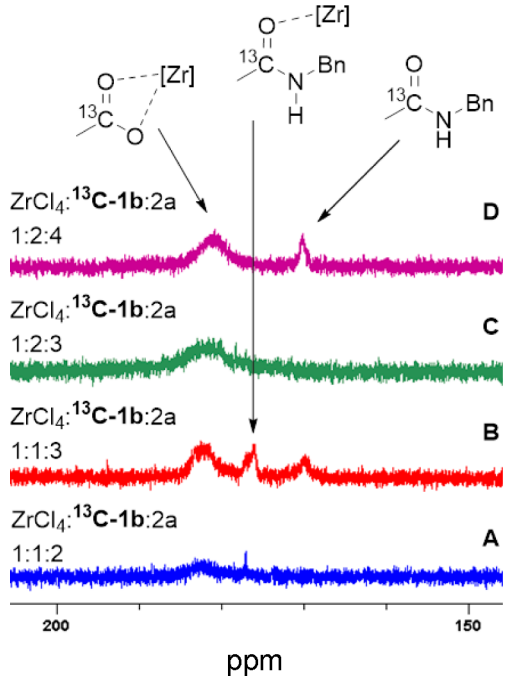

Figure 12. Amide product forms in the NMR experiments when amine is added to the zirconium carboxylate complexes.

compared to 2 equiv needed for the 1:1 mixture of $ZrCl_4$ and acetic acid ^{13}**C-1b** (Figure 11C). An interpretation of this observation is that the amine first acts as a base to deprotonate any HCl that results from the formation of the η^1-acetate complex from $ZrCl_4$ and acetic acid. When all HCl is consumed, the remaining amine ligates to zirconium and affords a change in carboxylate binding mode from η^1 to η^2. ^{1}H NMR examination of mixtures B–E in Figure 11 confirmed that zirconium-coordinated amine is present in all cases where the broad downfield peak is observed by ^{13}C NMR (see Supporting Information).

Figure 11A shows the ^{13}C NMR signal arising from the 1:1 mixture of ^{13}**C-1b** and $ZrCl_4$. The addition of 1 equiv of amine **2a** to the equimolar mixture results in the formation of a weak and broad signal downfield at 182.5 ppm (Figure 11B). By the addition of a second equivalent of **2a**, the broad downfield signal grows in intensity while the upfield peak at 171.5 ppm disappears (Figure 11C), suggesting a shift in carboxylate binding mode from monodentate to bidentate. This observation is consistent with previously reported zirconium complexes prepared under similar conditions.[31] In addition, a small peak appears at 176.4 ppm, corresponding to the zirconium-coordinated amide product ^{13}**C-3b** (for reference spectrum, see Supporting Information). The carbon signal at 171.5 ppm reappears upon the addition of a second equivalent of ^{13}**C-1b** (Figure 11D).

Amide product ^{13}**C-3b** forms upon addition of **2a** to the supposed η^2-zirconium acetate species that corresponds to the broad downfield ^{13}C NMR signal at 182.5 ppm. When 1 equiv of amine **2a** was added to a sample consisting of a 1:1:2 $ZrCl_4$/^{13}**C-1b**/**2a** mixture (Figure 12A), two new signals appeared, corresponding to the coordinated as well as the free amide product ^{13}**C-3b** (Figure 12B; see Supporting Information for reference spectrum). Similarly, the product peak was observed upon the addition of one amine equivalent to a 1:2:3 $ZrCl_4$/^{13}**C-1b**/**2a** sample (Figure 11C,D). This observation demonstrates that amide ^{13}**C-3b** can form from either a mono- or dicarboxylate zirconium complex in the presence of excess amine and hence that both of these complexes might be catalytically relevant. Product formation was also observed to occur in the 1:1:1 mixture of $ZrCl_4$, **2a**, and [^{13}**C-1b**]$^-$**Na**$^+$) upon the addition of one amine equivalent (see Supporting Information).

Consistent with reports for similar Lewis acid complexes,[25] ^{1}H NMR experiments demonstrate that benzylamine **2a** as well as *N*-benzylacetamide **3b** coordinate neutrally to zirconium in their respective 1:1 mixtures with $ZrCl_4$. The formation of amide product upon addition of the second and third amine equivalent per zirconium for the 1:1 mixtures of $ZrCl_4$/[^{13}**C-1b**]$^-$**Na**$^+$ and $ZrCl_4$/^{13}**C-1b**, respectively (vide infra) suggests that the amine ligates to the metal center in a 1:1 fashion. This conclusion is further supported by ^{1}H NMR titration experiments (see Supporting Information).

The NMR results from the sequential addition of ^{13}**C-1b** and amine **2a** to $ZrCl_4$ indicates that two carboxylates can ligate simultaneously to one zirconium center (Figure 11). This observation is consistent with the findings of Ludwig and Schwartz, who reported that two chloride ligands on $ZrCl_4$ are replaced by carboxylic acids already at 21 °C to form $ZrCl_2(OAc)_2$ with the loss of HCl.[32] Only at temperatures over 100 °C was full ligand exchange reported to occur, furnishing the 8-coordinated zirconium tetraacetate. Similarly, Mehrotra and Misra found that $ZrCl_2(OAc)_2$ readily formed from $ZrCl_4$ and *t*-butoxyacetate, whereas further substitution was unfavored at moderate temperature.[33]

Furthermore, it was reported that zirconium forms a dicarboxylate complex from $ZrCl_4$ and caproic acid under similar conditions.[31] The NMR study demonstrates that the

DOI: 10.1021/jacs.6b10973
J. Am. Chem. Soc. 2017, 139, 2286–2295

carboxylate carbon signals for zirconium-coordinated ^{13}**C-1b** broaden and move downfield to higher parts per million shifts upon the addition of $n_{(carboxylate)}$ + 1 amine equivalents, suggesting a shift in binding mode from monodentate to bidentate. Furthermore, it was found that both the complexes with one carboxylate and one amine ligand per zirconium as well as the complex with two carboxylates and one amine ligand per metal form amide product ^{13}**C-3b** in the presence of excess amine, indicating that they may be catalytically relevant. Despite several attempts, we were unable to obtain reliable results regarding the type of binding mode of the acetate as well as the nuclearity of the amide-forming zirconium complexes, using both high-resolution mass spectrometry (ESI-TOF) and in situ IR spectroscopy. This is consistent with previously reported problems for the isolation of single crystals for similar zirconium carboxylate compounds[25] and emphasizes the lability of the metal complexes.

2.4. Computational Study. To shed more light on the operating mechanism of the zirconium-catalyzed direct amidation, we turned our efforts to DFT calculations (see Supporting Information for computational details). Phenylacetic acid **1a** and benzylamine **2a** were used as model substrates. The experimental findings discussed above, combined with literature precedence, suggest that the active catalyst complex contains up to two carboxylate ligands per zirconium center, that the carboxylates coordinate to zirconium in a bidentate fashion, and that the metal complex contains one amine ligand per zirconium center. The starting zirconium complex was assumed to be $ZrCl_4(THF)_2$ with the two THF molecules in a *cis* configurations.[34]

Both mono- and dinuclear zirconium complexes that satisfy the above criteria can be envisioned, and we have optimized the geometries and calculated the energies relative to the starting materials for a number of these, as shown in Figure 13 (see

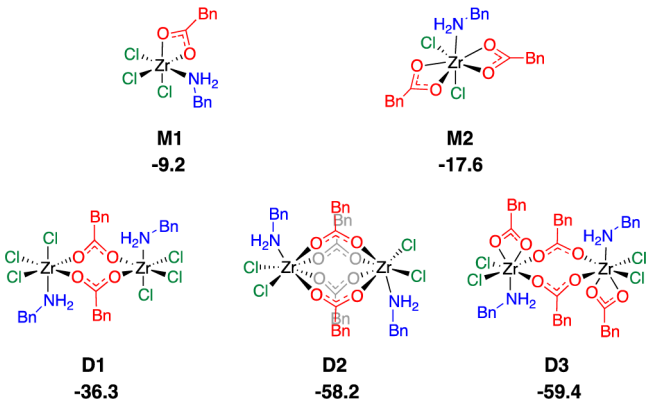

Figure 13. Possible complexes that can serve as the starting point for the catalytic cycle with their calculated free energies (in kcal/mol) relative to the starting material ($ZrCl_4(THF)_2$, **1a**, and **2a**).

Supporting Information for more details). It can be noted that structures **M2**, **D2**, and **D3** contain heptacoordinated zirconium centers. Even though zirconium generally adopts an octahedral coordination sphere, it is also known that it can form eight- as well as seven-coordinated complexes.[35−39]

We first note that the dinuclear complexes (**D1**−**D3**) are more stable than the mononuclear ones (**M1** and **M2**). Although the calculated formation energies can contain large inaccuracies (most importantly, due to inherent difficulties in the treatment of solvation and entropies), the obtained difference between mono- and dinuclear complexes indicates that the latter are a more likely scenario. It is known that dimeric centrosymmetric zirconium complexes of the type $[Zr(OR)_4(RNH_2)]_2$ with two bridging alkoxides form upon the addition of primary amine to the tetraalkoxide metal complex.[40] A similar dimeric structure has previously been suggested to be the active catalyst in zirconium-catalyzed amide formation of esters and amines,[41] and it has also been suggested that zirconium carboxylate complexes form dimers in solution with bridging carboxylate ligands.[42] The relative stability of the calculated dimers **D1**−**D3** is therefore not unexpected. We have calculated the catalytic cycle starting from the lowest-energy complex **D3** (Figures 14 and 15). Since the kinetic studies demonstrate a first-order rate dependence on zirconium concentration, the catalyst is assumed to maintain its nuclearity throughout the cycle.

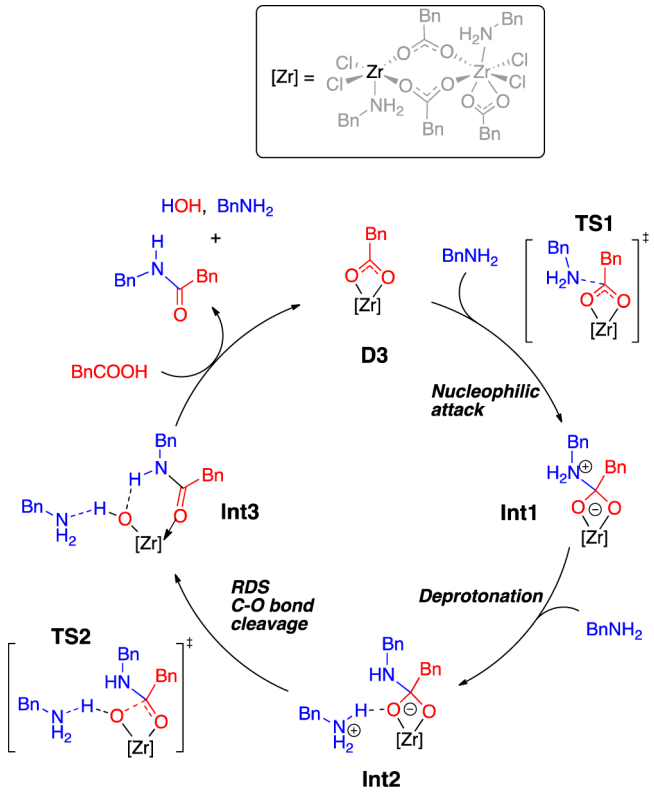

Figure 14. Calculated catalytic cycle starting from the dinuclear Zr complex **D3**.

The cycle starts with a nucleophilic attack of an external amine on the carboxylate carbon of a terminal acid (**TS1**), resulting in the tetrahedral intermediate **Int1**. The calculated barrier for this step is 10.7 kcal/mol, and the tetrahedral intermediate has the same energy. Next, a proton transfer takes place from **Int1** to another external amine, which then forms a hydrogen bond to the oxygen (**Int2**). This process is thermoneutral, as **Int2** has a very similar energy to **Int1**. The following step is a C−O bond cleavage coupled with a proton transfer from the external amine to the oxygen, forming the *cis* conformer of the amide and a zirconium-coordinated hydroxyl group (**Int3**). The transition state for this step (**TS2**) is 10.9 kcal/mol higher than **Int2**, that is, 21.6 kcal/mol relative to **D3**. To close the catalytic cycle and regenerate the **D3** complex, a new carboxylic acid has to enter and protonate the hydroxyl

DOI: 10.1021/jacs.6b10973
J. Am. Chem. Soc. 2017, 139, 2286−2295

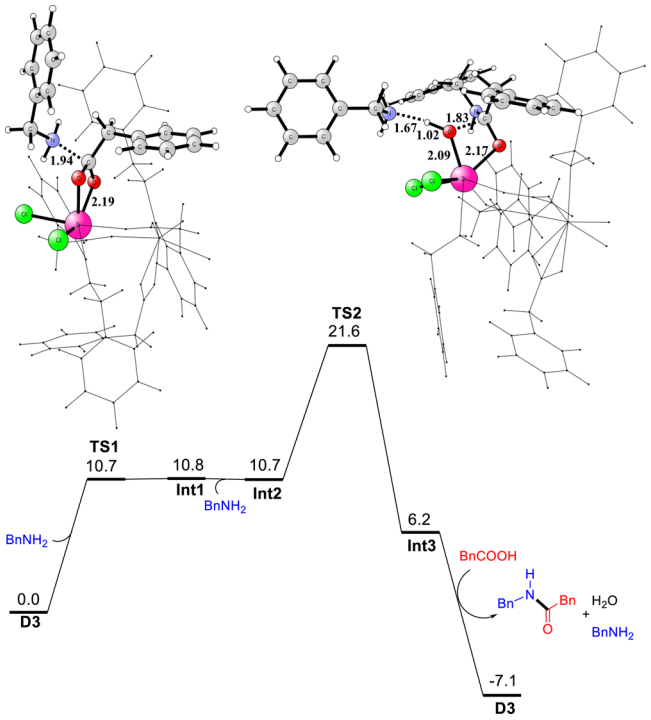

Figure 15. Calculated free energy graph for the catalytic cycle starting from dinuclear complex **D3**. The optimized structures of TS1 and TS2 are included.

group, which leaves as a water molecule along with the amide product. This process is calculated to be exergonic by 13.3 kcal/mol.

According to the calculated free energy profile for the **D3**-catalyzed amidation (Figure 15), the C−O bond cleavage (**TS2**) constitutes the turnover-limiting step of the reaction, resulting in a coordinated amide in *cis* conformation (**Int3**). This is analogous to what was previously determined for direct amidation catalyzed by boronic acids.[43,44] The predicted *cis* stereochemistry in the amide-forming step of the cycle can be rationalized by the hydrogen bonding interactions between the N−H proton and the zirconium-bound hydroxyl group. However, the amide is expected to isomerize to the energetically favored *trans* form when dissociated from the catalyst. The calculated overall barrier for the C−O bond cleavage is 21.6 kcal/mol, which is consistent with the experimental conditions.

The above calculations show that the dinuclear Zr complex **D3** can catalyze the direct amidation reaction with feasible energy barriers. It is interesting to note that the energy barrier for nucleophilic attack of an external amine at a bridging instead of a terminal carboxylate in **D3** is calculated to be higher (18.0 vs 10.7 kcal/mol). Furthermore, the subsequent C−O bond cleavage step is also higher in energy (25.0 vs 21.6 kcal/mol), thus making this scenario less likely. The higher barriers are likely the result of a higher extent of steric clashes because the environment around the brigding carboxylate is more crowded compared to the terminal one.

Calculations starting from the **D2** complex, which has a similar energy to **D3**, leads to **TS1** and **TS2** energies of 13.9 and 27.2 kcal/mol, respectively. The rate-limiting barrier for **D2** is thus significantly higher than that for **D3**, and **D2** is therefore considered to be less likely to represent the starting point of the catalytic cycle. Also in this case, sterics is likely to be the main reason for the higher barriers.

For comparison, we have also computed the full catalytic cycles starting from the less stable complexes **M1**, **M2**, and **D1** (Figure 13). Very similar reaction steps were obtained but with significant differences in the energy profiles (see Supporting Information for details).

Starting from the **D3** structure, we have also considered the reaction of unsubstituted and 4-chloro- and 4-methoxy-substituted benzoic acids. The calculations could nicely reproduce the observed substituent effects shown in Figure 9 with faster reaction rates for benzoic acids that have electron-withdrawing substituents and slower rates for those with electron-donating groups. The rate-limiting barrier for 4-chlorobenzoic acid is calculated to be 0.9 kcal/mol lower than unsubstituted benzoic acid, whereas the barrier for 4-methoxybenzoic acid was calculated to be 0.6 kcal/mol higher (see Supporting Information). These results lend thus further support to the suggested reaction mechanism of Figure 14.

Finally, a few words about the catalyst−carboxylic acid off-cycle species. As mentioned above, it is not possible to determine the nature of this species based on NMR experiments. However, one could use DFT calculations to speculate on possible structures. The negative rate dependence on [carboxylic acid] indicates that the off-cycle species contains more acid per zirconium compared to the active catalyst. By optimizing the geometries of a number of conceivable structures and evaluating their energies, we could identify one dimeric structure with lower energy compared to those shown in Figure 13. The species contains three carboxylates per metal ion and is calculated to be about 13 kcal/mol lower than **D3**. The structure and energy of the calculated species are found in Supporting Information.

3. CONCLUSIONS

Herein, we present a detailed mechanistic study of the zirconium-catalyzed amidation of carboxylic acids and amines using kinetics, NMR spectroscopy, and DFT calculations. The reaction is found to be first order with respect to catalyst concentration and to display positive rate dependence on amine and negative rate dependence on carboxylic acid concentration. The latter, combined with the reaction's sigmoidal profile under synthetically relevant conditions, indicate that reversible catalyst−carboxylic acid off-cycle species are formed under the reaction conditions. "Same excess" experiments demonstrate both that the catalyst is sensitive toward product inhibition and that the inhibition can be avoided by the use of a larger excess amine. Furthermore, the same excess experiments conclusively shows that irreversible catalyst deactivation does not occur. Electron-withdrawing groups on the carboxylic acid were found to enhance the reaction rate, whereas electron-donating groups resulted in slower amide formation. These findings suggest that the energy barrier for the turnover-limiting step of the catalytic cycle is lowered by electron-withdrawing substituents and that electron-donating groups destabilize the same step. NMR studies suggest that product-forming complexes contain one or two bidentate carboxylate ligands and one neutral amine ligand per zirconium and serve as the basis for a theoretical study of the catalytic cycle using DFT calculations. These calculations demonstrate that a symmetric dimer can catalyze the amide formation with feasible energy barriers. The C−O bond cleavage is identified as the turnover-limiting step, and it is

DOI: 10.1021/jacs.6b10973
J. Am. Chem. Soc. 2017, 139, 2286−2295

indicated that the proton transfer from N to O in the tetrahedral intermediate is mediated by an external amine. Furthermore, the calculations reproduce the experimentally observed effects on reaction rate by electronically different substituents on the carboxylic acid.

The combined results of this study provide unprecedented insight into the mechanistic action of zirconium-catalyzed direct amidation and led to the design of a more efficient reaction protocol, resulting in increased isolated yields and lower catalyst loadings. These improvements are highly valuable for the competitiveness of this catalytic methodology as an alternative to the use of coupling reagents and other stoichiometric activation methods for amide synthesis. The rate dependencies on carboxylic acid and amine, as well as the impact on reaction rate by electron-withdrawing groups on the carboxylic acid, were found to be the opposite of systems that employ boron-based catalysts.[7a,b,45] These findings indicate that the zirconium-catalyzed system operates quite differently compared to the boron-based systems and suggest that complementary use of the two catalyst types may result in synthetic benefits. The importance of the amine for several aspects of the zirconium-catalyzed amidation stands out in this study. A focus on this reaction component will likely open further development of efficient reaction protocols as well as the development of new catalysts of this class.

■ ASSOCIATED CONTENT

Supporting Information

The Supporting Information is available free of charge on the ACS Publications website at DOI: 10.1021/jacs.6b10973.

Experimental procedures, Burés graphical analysis, same excess experiments, NMR studies and computational studies (PDF)

■ AUTHOR INFORMATION

Corresponding Authors

*fahmi.himo@su.se

*hans.adolfsson@umu.se

ORCID

Fredrik Tinnis: 0000-0003-1271-4601

Andrés G. Algarra: 0000-0002-5062-2858

Fahmi Himo: 0000-0002-1012-5611

Author Contributions

⊥F.T. and J.Z. contributed equally.

Notes

The authors declare no competing financial interest.

■ ACKNOWLEDGMENTS

The authors gratefully acknowledge Professor Donna G. Blackmond for valuable comments and suggestions on the experimental section, Kristina Romare for assistance with NMR experiments, and The K & A Wallenberg Foundation and the Swedish Research Council for financial support.

■ REFERENCES

(1) (a) Beringer, M.; Rodnina, M. V. *Mol. Cell* **2007**, *26*, 311−321. (b) Polacek, N.; Mankin, A. S. *Crit. Rev. Biochem. Mol. Biol.* **2005**, *40*, 285−311.

(2) Eisenberg, D. D.; Gill, H. S.; Pfluegl, G. M. U.; Rotstein, S. H. *Biochim. Biophys. Acta, Protein Struct. Mol. Enzymol.* **2000**, *1477*, 122−145.

(3) Carey, J. S.; Laffan, D.; Thomson, C.; Williams, M. T. *Org. Biomol. Chem.* **2006**, *4*, 2337−2347.

(4) Dunetz, J. R.; Magano, J.; Weisenburger, G. A. *Org. Process Res. Dev.* **2016**, *20*, 140−177.

(5) (a) Constable, D. J. C.; Dunn, P. J.; Hayler, J. D.; Humphrey, G. R.; Leazer, J. L., Jr.; Linderman, R. J.; Lorenz, K.; Manley, J.; Pearlman, B. A.; Wells, A.; Zaks, A.; Zhang, T. Y. *Green Chem.* **2007**, *9*, 411−420. (b) Bandichhor, R.; Bhattacharya, A.; Diorazio, L.; Dunn, P.; Fraunhoffer, K.; Gallou, F.; Hayler, J.; Hickey, M.; Hinkley, B.; Hughes, D.; Humphreys, L.; Kaptein, B.; Mathew, S.; Oh, L.; Richardson, P.; White, T.; Wuyts, S. *Org. Process Res. Dev.* **2013**, *17*, 1394−1405.

(6) (a) Allen, C. L.; Williams, J. M. J. *Chem. Soc. Rev.* **2011**, *40*, 3405−3415. (b) de Figueiredo, R. M.; Suppo, J.-S.; Campagne, J.-M. *Chem. Rev.* **2016**, *116*, 12029−12122.

(7) (a) Arnold, K.; Davies, B.; Giles, R. L.; Grosjean, C.; Smith, G. E.; Whiting, A. *Adv. Synth. Catal.* **2006**, *348*, 813−820. (b) Charville, H.; Jackson, D. A.; Hodges, G.; Whiting, A.; Wilson, M. R. *Eur. J. Org. Chem.* **2011**, *2011*, 5981−5990. (c) Allen, C. L.; Chhatwal, A. R.; Williams, J. M. J. *Chem. Commun.* **2012**, *48*, 666−668. (d) Grosjean, C.; Parker, J.; Thirsk, C.; Wright, A. R. *Org. Process Res. Dev.* **2012**, *16*, 781−787. (e) Rahman, M.; Kundu, D.; Hajra, A.; Majee, A. *Tetrahedron Lett.* **2010**, *51*, 2896−2899.

(8) Lundberg, H.; Tinnis, F.; Selander, N.; Adolfsson, H. *Chem. Soc. Rev.* **2014**, *43*, 2714−2742.

(9) (a) Gu, L.; Lim, J.; Cheong, J. L.; Lee, S. S. *Chem. Commun.* **2014**, *50*, 7017−7019. (b) Mohy El Dine, T.; Erb, W.; Berhault, Y.; Rouden, J.; Blanchet, J. *J. Org. Chem.* **2015**, *80*, 4532−4544. (c) El Dine, T. M.; Rouden, J.; Blanchet, J. *Chem. Commun.* **2015**, *51*, 16084−16087. (d) Tam, E. K. W.; Rita; Liu, L. Y.; Chen, A. *Eur. J. Org. Chem.* **2015**, *2015*, 1100−1107. (e) Ali, Md. A.; Siddiki, S. M. A. H.; Onodera, W.; Kon, K.; Shimizu, K.-i. *ChemCatChem* **2015**, *7*, 3555−3562.

(10) Lundberg, H.; Tinnis, F.; Adolfsson, H. *Synlett* **2012**, *23*, 2201−2204.

(11) (a) Lundberg, H.; Tinnis, F.; Adolfsson, H. *Chem. - Eur. J.* **2012**, *18*, 3822−3826. (b) Tinnis, F.; Lundberg, H.; Adolfsson, H. *Adv. Synth. Catal.* **2012**, *354*, 2531−2536.

(12) Lundberg, H.; Adolfsson, H. *ACS Catal.* **2015**, *5*, 3271−3277.

(13) Burés, J. *Angew. Chem., Int. Ed.* **2016**, *55*, 2028−2031.

(14) (a) Tokunaga, M.; Larrow, J. F.; Kakiuchi, F.; Jacobsen, E. N. *Science* **1997**, *277*, 936−938. (b) Ford, D. D.; Nielsen, L. P.; Zuend, S. J.; Musgrave, C. B.; Jacobsen, E. N. *J. Am. Chem. Soc.* **2013**, *135*, 15595−15608. (c) Nielsen, L. P. C.; Stevenson, C. P.; Blackmond, D. G.; Jacobsen, E. N. *J. Am. Chem. Soc.* **2004**, *126*, 1360−1362.

(15) (a) Blackmond, D. G. *Angew. Chem., Int. Ed.* **2005**, *44*, 4302−4320. (b) Blackmond, D. G. *J. Am. Chem. Soc.* **2015**, *137*, 10852−10866.

(16) Baxter, R. D.; Sale, D.; Engle, K. M.; Yu, J.-Q.; Blackmond, D. G. *J. Am. Chem. Soc.* **2012**, *134*, 4600−4606.

(17) (a) Clearfield, A. *Rev. Pure. Appl. Chem.* **1964**, *14*, 91−108. (b) Johnson, J. S.; Kraus, K. A. *J. Am. Chem. Soc.* **1956**, *78*, 3937−3943.

(18) Sung, S.; Sale, D.; Braddock, D. C.; Armstrong, A.; Brennan, C.; Davies, R. P. *ACS Catal.* **2016**, *6*, 3965−3974.

(19) Hein, J. E.; Armstrong, A.; Blackmond, D. G. *Org. Lett.* **2011**, *13*, 4300−4303.

(20) Rosner, T.; Le Bars, J.; Pfaltz, A.; Blackmond, D. G. *J. Am. Chem. Soc.* **2001**, *123*, 1848−1855.

(21) Ferretti, A. C.; Brennan, C.; Blackmond, D. G. *Inorg. Chim. Acta* **2011**, *369*, 292−295.

(22) Zotova, N.; Franzke, A.; Armstrong, A.; Blackmond, D. G. *J. Am. Chem. Soc.* **2007**, *129*, 15100−15101.

(23) Seebach, D.; Beck, A. K.; Badine, D. M.; Limbach, M.; Eschenmoser, A.; Treasurywala, A. M.; Hobi, R. *Helv. Chim. Acta* **2007**, *90*, 425−471.

(24) Arena, F.; Deiana, C.; Lombardo, A.; Ivanchenko, P.; Sakhno, Y.; Trunfio, G.; Martra, G. *Catal. Sci. Technol.* **2015**, *5*, 1911−1918.

(25) (a) Clearfield, A. *Rev. Pure Appl. Chem.* **1964**, *14*, 91−108. (b) Joshi, K.; Bao, J.; Goldman, A. S.; Kohn, J. *J. Am. Chem. Soc.* **1992**, *114*, 6649−6652.

DOI: 10.1021/jacs.6b10973
J. Am. Chem. Soc. 2017, 139, 2286−2295

(26) (a) Makhaev, V. D.; Matkovskii, P. E.; Petrova, L. A.; Sasnovskaya, V. D. *Russ. Chem. Bull.* **2010**, *59*, 1735−1739. (b) Zhou, Y.-K.; Chen, H.-M. *Polyhedron* **1990**, *9*, 2689−2691.
(27) Mukherjee, S.; Datta, A. *Phys. Rev. E* **2011**, *84*, 041601.
(28) Suzuki, H.; Takiguchi, T.; Kawasaki, Y. *Bull. Chem. Soc. Jpn.* **1978**, *51*, 1764−1767.
(29) Dixit, S. C.; Sharan, R.; Kapoor, R. N. *Inorg. Chim. Acta* **1989**, *158*, 109−113.
(30) Abu Ali, H.; Omar, S. N.; Darawsheh, M. D.; Fares, H. *J. Coord. Chem.* **2016**, *69*, 1110−1122.
(31) Refat, M. S.; El-Korashy, S. A.; Kumar, D. N.; Ahmed, A. S. *Spectrochim. Acta, Part A* **2008**, *70*, 217−233.
(32) Ludwig, J.; Schwartz, D. *Inorg. Chem.* **1970**, *9*, 607−611.
(33) Mehrotra, R. C.; Misra, R. A. *J. Chem. Soc.* **1965**, 43−46.
(34) Eberle, M.; Röhr, C. *Acta Crystallogr.* **1996**, *52*, 552−556.
(35) Fric, H.; Puchberger, M.; Schubert, U. *Eur. J. Inorg. Chem.* **2008**, *2008*, 1452−1461.
(36) Payne, P. R.; Thomson, R. K.; Medeiros, D. M.; Wan, G.; Schafer, L. L. *Dalton Trans.* **2013**, *42*, 15670−15677.
(37) Leitch, D. C.; Payne, P. R.; Dunbar, C. R.; Schafer, L. L. *J. Am. Chem. Soc.* **2009**, *131*, 18246−18247.
(38) Willey, G.; Woodman, T.; Fisher, M.; Drew, M. B. *Transition Met. Chem.* **1998**, *23*, 467−471.
(39) Hart, R.; Levason, W.; Patel, B.; Reid, G. *J. Chem. Soc., Dalton Trans.* **2002**, 3153−3159.
(40) Fric, H.; Puchberger, M.; Schubert, U. *J. Sol-Gel Sci. Technol.* **2006**, *40*, 155−162.
(41) Han, C.; Lee, J. P.; Lobkovsky, E.; Porco, J. A., Jr. *J. Am. Chem. Soc.* **2005**, *127*, 10039−10044.
(42) Schwartz, D.; Johnson, C.; Ludwig, J.; Morris, M. L. *J. Inorg. Nucl. Chem.* **1964**, *26*, 2025−2027.
(43) Marcelli, T. *Angew. Chem., Int. Ed.* **2010**, *49*, 6840−6843.
(44) Wang, C.; Yu, H.-Z.; Fu, Y.; Guo, Q.-X. *Org. Biomol. Chem.* **2013**, *11*, 2140.
(45) Al-Zoubi, R. M.; Marion, O.; Hall, D. G. *Angew. Chem., Int. Ed.* **2008**, *47*, 2876−2879.

DOI: 10.1021/jacs.6b10973
J. Am. Chem. Soc. 2017, 139, 2286−2295